



Room temperature magnetocaloric effect of La-deficient bulk perovskite manganite $\text{La}_{0.7}\text{MnO}_{3-\delta}$

Zhiming Wang^{a,c,*}, Qingyu Xu^b, Jingzhi Sun^d, Jian Pan^e, He Zhang^a

^a Institute of Mechanical Engineering, Nanjing University of Science and Technology, Xiaolingwei 200, Xuanwu District, Nanjing City 210094, China

^b Physics Department of Southeast University, Sipailou 2 Xuanwu District, Nanjing 211189, China

^c Laboratory of Solid State Microstructures, Nanjing University, 22 Hankou Road, Gulou District, Nanjing 210093, China

^d Key Laboratory of Silicon Materials, Zhejiang University, Zheda Road 38, West Lake District, Hangzhou 310027, China

^e Department of Physics, Fudan University, Handan Road 220 Yangpu District, Shanghai 200433, China

ARTICLE INFO

Article history:

Received 2 September 2010

Received in revised form

11 January 2011

Accepted 20 January 2011

Available online 26 January 2011

Keywords:

Perovskite manganite

Magnetocaloric effect

ABSTRACT

Room temperature magnetocaloric effect in La-deficient bulk perovskite manganite $\text{La}_{0.7}\text{MnO}_{3-\delta}$ prepared by conventional solid-state reaction has been reported. The maximum value of the magnetic entropy change (about -1.32 J/kg K) and the refrigerant capacity (approximately close to 37 J/kg) had been obtained at 290 K corresponding to a magnetic field variation of 1 T for $\text{La}_{0.7}\text{MnO}_{3-\delta}$. It is the strong Jahn–Teller coupling that changes Mn–O bond length and Mn–O–Mn bond angles and then the canted spin arrangement and induces the strong double-exchange coupling to a comparatively high magnetic transition temperature. This Curie temperature near room temperature with easy fabrication and higher chemical stability makes $\text{La}_{0.7}\text{MnO}_{3-\delta}$ a potential candidate as a working substance in magnetic refrigeration technology.

© 2011 Elsevier B.V. All rights reserved.

Recently, increasing interest has been focused on the large magnetocaloric (MC) effect in the perovskite manganites (ABO_3) $\text{Ln}_{1-x}\text{T}_x\text{MnO}_3$ ($\text{Ln}=\text{La}^{3+}, \text{Nd}^{3+}, \text{Pr}^{3+}$, etc., $\text{T}=\text{Ca}^{2+}, \text{Sr}^{2+}, \text{Ba}^{2+}$, etc.), owing to its many advantages on gas refrigeration: low noise, softer vibration, longer usage time, absence of freon, etc. [1–7]. So far, much attention in experiment has been paid to find refrigerants that have large magnetic entropy change under magnetic field change that can especially be used at room temperature. In perovskite manganites, the large MC effect has been observed near the ferromagnetic transition temperature (i.e. Curie temperature) T_C [3–13]. When a field is applied, the unpaired spins are aligned parallel to the field in these materials, which lowers the entropy and causes the sample to heat up. On the contrary, when an applied field is removed from a magnetic sample, the spin tends to become random, which increases the entropy and causes the material to cool off. Therefore, MC effect in this kind of material always occurs at its magnetic ordering temperature (i.e. T_C). Among them, $\text{La}_{0.67}\text{Ca}_{0.33}\text{MnO}_3$ is the most attractive material because T_C (~ 250 K) is near room temperature and the large magnetic entropy change of 0.5 J/kg K under 1 T magnetic field at T_C . However, T_C of $\text{La}_{0.67}\text{Ca}_{0.33}\text{MnO}_3$ is still lower than room temperature [14–15]. To utilize MC properties at low field and around room temperature,

some effort has been made to promote T_C to room temperature by fine tuning the average A-site cation radius $\langle r_A \rangle$ [16]. Other effort has been made to explore double-exchange mechanism by partial change the content of oxygen [17–22]. In this paper, we report magnetocaloric effect of a special perovskite manganite – $\text{La}_{0.7}\text{MnO}_{3-\delta}$ – at room temperature ($T_C \sim 290$ K).

In order to excite double-exchange effect, La-deficient type $\text{La}_{0.7}\text{MnO}_{3-\delta}$ bulk perovskite manganite was deliberately prepared pro rata by conventional solid-state reaction processing. Appropriate amounts of high-purity La_2O_3 and MnCO_3 powders were mixed and ground, then pressed into disks at a pressure of 250 MPa and presintered at 900 °C for 10 h. After that, the disks were broken, ground, and pressed into disks of 10 mm in diameter at 250 MPa, and subsequently sintered for 10 h at 1100 °C inside the Muffle furnace. The crystal structure of the bulk was determined by an X-ray diffractometer (XRD) using a D/max-rA diffractometer (made by Rigaku Corp.) with the CuK_α radiation and a graphite monochromator. Mn^{4+} content was examined by the oxidation–reduction titration (29.2% in 5% error range, then δ is 0.303 for the La vacancies in oxygen nonstoichiometry, the experimental Mn^{4+} concentration is coincident with other experimental and the theoretical values [23–25], the rhombohedral structure of the compositions supports the high value of the Mn^{4+} content [24–25]). M – T and M – H curves were measured using a vibrating sample magnetometer (VSM, LakeShore Cryotronics, Inc.). T_C was determined from M – T curves. The phase transition was measured by differential scanning calorimeter (DSC, Rigaku PTC-10A).

* Corresponding author at: Institute of Mechanical Engineering, Nanjing University of Science and Technology, Xiaolingwei 200, Xuanwu District, Nanjing City 210094, China. Tel.: +86 25 84318429; fax: +86 25 84315694.

E-mail address: zhimingwang@mail.njust.edu.cn (Z. Wang).

La-deficiency and oxygen nonstoichiometry suggest that the perovskite type oxides with a mixed valence of Mn³⁺ and Mn⁴⁺ lead to the changes in the structural, electronic transport, and physical properties, which is responsible for the occurrence of both ferromagnetic behavior and magnetocaloric effect. Series of investigations in the La_{1-x}MnO_{3-δ} show that above-mentioned properties strongly depend on *x* and *δ*. Until now MC effect about the critical temperature 293 K ascribed to the self-doping is not adequately reported.

Fig. 1 displays the X-ray diffraction (XRD) pattern of polycrystalline bulk sample La_{0.7}MnO_{3-δ}. The results of X-ray diffraction display almost single structural rhombohedral phase in our samples of self-doped manganese perovskites (the peak corresponding to MnO₂ and Mn₃O₄ had been not observed from XRD). Magnetization was measured using a vibrating sample magnetometer with an absolute accuracy of 5 × 10⁻⁵ emu. A sample was placed inside a polyethylene pipe. The temperature dependence of low field magnetization for La_{0.7}MnO_{3-δ}, shown in Fig. 2, was measured in a wide range of temperature (from 100 up to 320 K) in applied field of 0.1 T in order to determine ferromagnetic ordering transition (i.e. spin-ordering) temperature *T*_C of the materials. *T*_C, defined as the temperature at which the

∂M/∂T–*T* curve reaches a minimum, have been determined from *M*–*T* curves.

Shown in Fig. 3 is magnetization versus applied field obtained at various temperatures for La_{0.7}MnO_{3-δ} sample. In our experiments, the changing rate of applied field is slow enough to get isothermal *M*–*H* curves.

The magnetic entropy change that results from the spin-ordering (i.e. ferromagnetic ordering) and is induced by the variation of the applied magnetic field from 0 to *H*_{max}, is given by

$$\Delta S_H = \int_0^{H_{\max}} \left(\frac{\partial M(H,T)}{\partial T} \right)_H dH \quad (1)$$

where *H*_{max} is the maximum external field. According to Eq. (1), magnetic entropy change depends on the temperature-gradient of magnetization and attains a maximum value around Curie temperature *T*_C at which magnetization decays rapidly.

In fact, the magnetic entropy change Δ*S*_H is often evaluated by some numerical approximation methods. One way of approximation is to directly use the adiabatic measurements of *M*–*T* curve

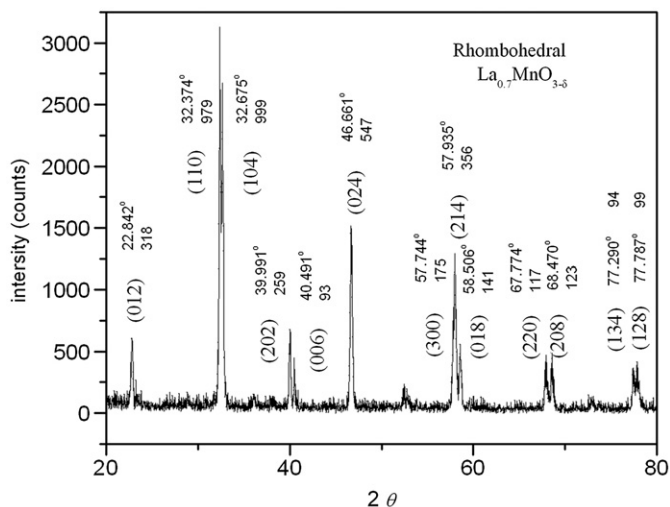


Fig. 1. X-ray diffraction pattern for the polycrystalline sample La_{0.7}MnO_{3-δ}.

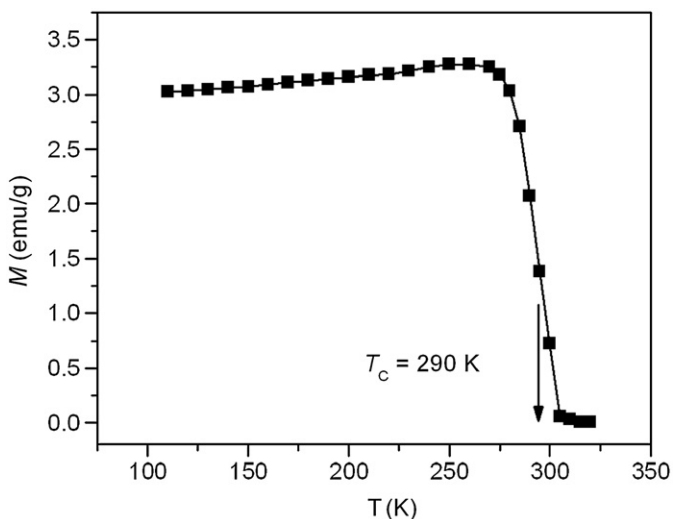


Fig. 2. Temperature dependence of magnetization for La_{0.7}MnO_{3-δ} sample obtained in a magnetic field of 0.1 T.

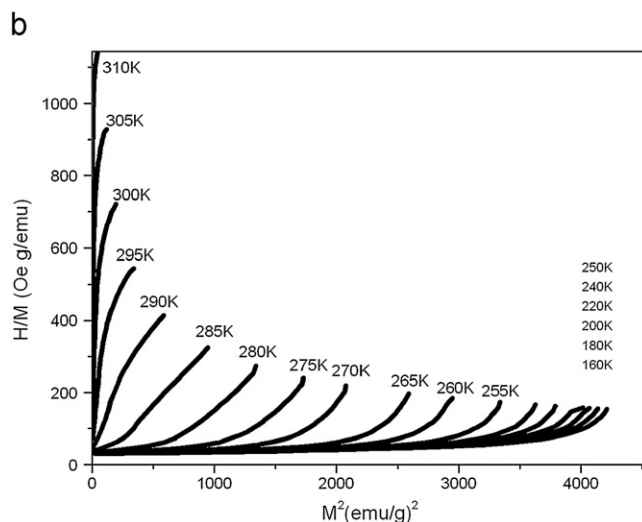
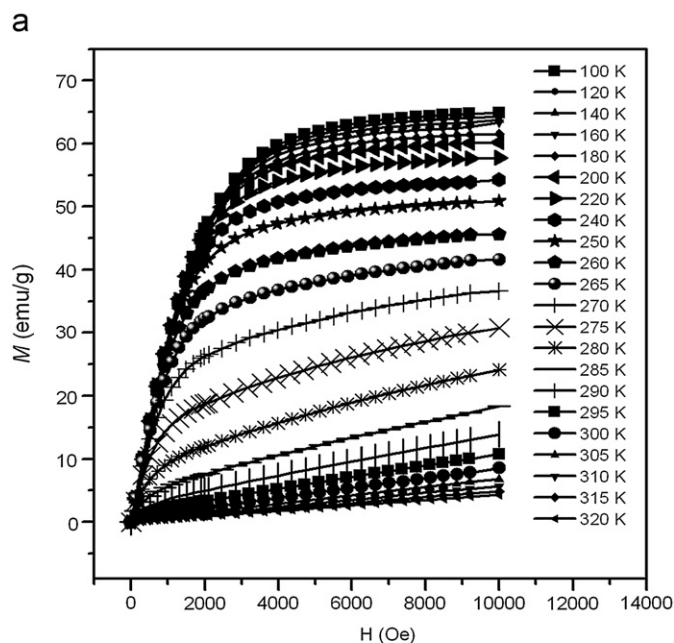


Fig. 3. (a) Isothermal magnetizations of sample as a function of applied near Curie temperature. The temperature step is 5 K in the region from 260 to 320 K. (b) *H*/*M* vs. *M*² plots of isotherms in the vicinity of the Curie temperature.

under different magnetic fields. In the case of small discrete field intervals, ΔS_H can be approximated from Eq. (1) as

$$\Delta S_H = \sum_i \left[\left(\frac{\partial M}{\partial T} \right)_{H_i} + \left(\frac{\partial M}{\partial T} \right)_{H_{i+1}} \right] \frac{1}{2} \Delta H_i \quad (2)$$

where $(\partial M/\partial T)_{H_i}$ is the experimental value obtained from M - T curve in magnetic field H_i . Another method is to use isothermal magnetization measurements. In the case of magnetization measurements at small discrete fields and temperature intervals, ΔS_H can be approximated from Eq. (1) by

$$\Delta S_H = \sum_i \frac{M_i - M_{i+1}}{T_{i+1} - T_i} \Delta H_i \quad (3)$$

The magnetic entropy changes associated with applied field variations had been calculated using Eq. (3). Fig. 4 shows the temperature dependence of magnetic entropy change for our sample. As expected from original Eq. (1), the peak of magnetic entropy changes is near T_C , where the variation of magnetization with temperature is the fastest. The maximum value of the magnetic entropy change corresponding to a magnetic field variation of 1 T for the $\text{La}_{0.7}\text{MnO}_{3-\delta}$ is about -1.32 J/kg K. It is clear that the magnetic entropy change in $\text{La}_{0.7}\text{MnO}_{3-\delta}$ originates from the considerable change of magnetization near T_C .

From a cooling perspective, it is important to consider not only the magnitude of the magnetic entropy change but also the refrigerant capacity (RC) that depends on both the magnetic entropy change and its temperature dependence.

The magnetic cooling efficiency of a magnetocaloric material can be, in simple cases, evaluated by considering the magnitude of ΔS_H and its full-width at half maximum (δT_{FWHM}) [26–28]. It is easy to establish the product of the ΔS_H maximum and the full-width at half maximum ($\delta T_{FWHM} = T_2 - T_1$) as

$$RCP = -\Delta S_H(T, H) \delta T_{FWHM}$$

which stands for the so-called relative cooling power (RCP) based on the magnetic entropy change. In this sample, 37 J/kg RCP is figured out.

In addition, the thermal and field hysteresis losses in magnetocaloric materials should also be considered in materials with first-order magnetic phase transitions especially in high magnetic

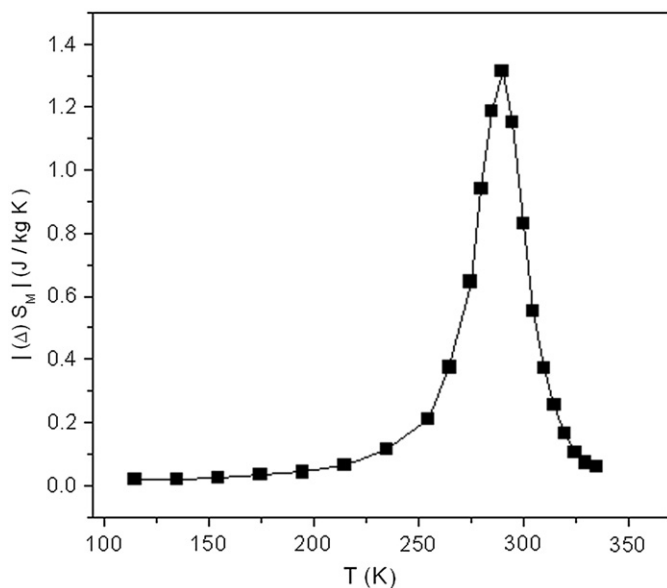


Fig. 4. Magnetic entropy change of $\text{La}_{0.7}\text{MnO}_{3-\delta}$ at a magnetic field $\mu_0 H = 1$ T as a function of temperature.

field. The field hysteresis losses cost in energy were used to make one cycle of the magnetic field when calculating RC of a magnetic refrigerant material being subjected to field cycling. It had been calculated that the influence of hysteretic losses is small in the perovskites manganites material at 1 T magnetic field and RCP is approximately close to RC with thermal/field hysteresis losses [29].

An endothermic DSC peak around T_C was observed during heating up measurement (shown in Fig. 5), indicating that this phase transition is of first-order, so that large magnetic entropy changes occur in the material. Regarding the character of a first-order or second-order phase transition, one of the simplest ways to determine is use of the Banerjee criteria in 1964 by analyzing H/M vs. M^2 curves. Banerjee detected the essential similarity between the Laudau–Lifshitz and Bean–Rodbell criteria and condensed them into one that provides a tool to distinguish first-order magnetic transitions from second-order ones by purely magnetic methods. It consists on the observation of the slope of isotherm plots of H/M vs. M^2 . A negative slope indicates a first-order transition. Fig. 3(b) shows H/M vs. M^2 plots of Fig. 3(a) isotherms in the vicinity of the Curie temperature. The negative sign of the slope for some temperatures from positive sign denoting the second-order character of the phase transition is clear [30–31]. Table 1 lists the data of several magnetic materials of perovskite manganite as comparisons.

The LaMnO_3 stoichiometry phase is characterized by a long-range A-type antiferromagnetic order, linked to superexchange between the Mn^{3+} pairs with the transition temperature T_N of 140 K [39]. Usually, the modification of La vacancies in oxygen nonstoichiometry or the divalent alkali ions injection of this phase to introduce Mn^{4+} , results in the double-exchange interaction occurred between the moments of the Mn^{4+} and those of its first Mn^{3+} neighbors associated with Mn^{3+} - Mn^{4+} pairs embedded in the Mn^{3+} - Mn^{3+} antiferromagnetic matrix. The Mn^{3+} - Mn^{4+} ferromagnetic cluster acts like an exchange between its neighboring top and bottom planes, whose moments point along the same direction as the net moment of the Mn^{3+} - Mn^{4+} cluster does. It is also interesting to indicate the fact that the destabilization of the antiferromagnetic structure (measurable field variation of Curie temperature T_C i.e. ferromagnetic ordering transition temperature) is related to the concentration of Mn^{4+} due to La vacancies in oxygen nonstoichiometry or alkali ions substitution in part. With or without vacancies, the structures of the perovskites are determined first by the lattice parameters, relative equilibrium bond

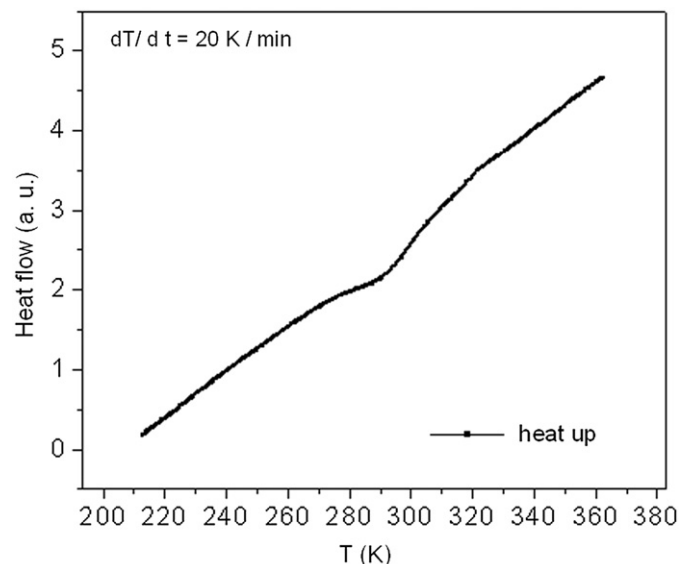


Fig. 5. DSC curve of $\text{La}_{0.7}\text{MnO}_{3-\delta}$ at heat up.

Table 1Curie temperature T_C , magnetic field H_{\max} , and the maximum entropy change $|\Delta S_H(T)|$ for several typical magnetic refrigeration materials.

| No. | Composition | Curie temperature(K) | Magnetic field H_{\max} (10 kOe) | Entropy change $ \Delta S_H(T) _{\max}$ (J/Kg K) | Ref. |
|-----|--|----------------------|-------------------------------------|--|-----------|
| 1 | $\text{La}_{0.7}\text{MnO}_{3-\delta}$ | 290 | 1 | 1.32 | This work |
| 2 | $\text{La}_{0.67}\text{Ca}_{0.33}\text{MnO}_3$ | 250 | 1 | 0.5 | [14] |
| 3 | $\text{La}_{2/3}\text{Ca}_{1/3}\text{MnO}_3$ | 267 | 3 | 6.4 | [15] |
| 4 | $\text{La}_{0.8}\text{Ca}_{0.2}\text{MnO}_3$ | 230 | 1.5 | 5.5 | [3] |
| 5 | $\text{La}_{0.6}\text{Ca}_{0.4}\text{MnO}_3$ | 263 | 3 | 5.0 | [13] |
| 6 | $\text{La}_{0.67}\text{Ca}_{0.33}\text{MnO}_\delta$ | 260 | 1 | 1.1 | [17] |
| 7 | $\text{La}_{0.60}\text{Y}_{0.07}\text{Ca}_{0.33}\text{MnO}_\delta$ | 230 | 1 | 0.55 | [17] |

lengths, and canted spin arrangement. The transition to the ferromagnetic ordering state is always accompanied by large changes in structures, which are compatible with the cooperative Jahn–Teller effect, and a corresponding polarization of e_g electron orbitals to definite planes, in which a strong Jahn–Teller effect is involved, which cooperatively order the e_g orbitals of Mn^{3+} ions.

This is governed by ferromagnetic interactions of double-exchange interaction origin pointing to a fast electron transfer between Mn ions [25]. It agrees with the general correlation between the cooperative Jahn–Teller deformation in the rhombohedral phase and strengths of the double-exchange ferromagnetic coupling in Mn perovskites. There is a gradual increase in the Curie temperature, which correlates with the increasing width of the electronic e_g band.

And the large value of the electron–phonon coupling is also clear in the regime of the manganites, where a static Jahn–Teller distortion plays a key role in the physics of the material. La vacancies in oxygen nonstoichiometry distribution of this phase to introduce Mn^{4+} urge the dynamic Jahn–Teller coupling between an e_g orbital and the surrounding O^{2-} octahedron. Millis et al. [40] thought that a dynamical Jahn–Teller effect may persist at higher hole densities from La-deficiency and oxygen nonstoichiometry, without leading to long-range order but producing important fluctuations that localize electrons by splitting the degenerate e_g levels at a given MnO_6 octahedron [32].

In the series of La vacancies samples [33–35] and this sample $\text{La}_{0.7}\text{MnO}_{3-\delta}$, $\text{MnO}_{3-\delta}$ array is perturbed by the oxygen nonstoichiometry, with the strong Jahn–Teller effect that traps Mn^{3+} ions [25], so the 29.2% Mn^{4+} ions via double-exchange interaction are more mobile and the canting of the spin also increases with Mn^{4+} content, then result in increased T_C to 290 K [25,37–38]. On contrary, $T_C=254$ K in $\text{La}_{0.9}\text{MnO}_{2.97}$ samples where a few Mn^{4+} ions with lower average number of Mn^{3+} – Mn^{4+} pairs originate by the occurrence of broken bonds (calculated about 24% on the discuss of reference paper [36]) in the case of comparatively weakly dynamic Jahn–Teller coupling and comparatively degenerated e_g levels at the MnO_6 octahedron.

When an applied field is applied to this kind of manganites material, the unpaired spins are aligned parallel to the field. Since the total entropy of spins plus the lattice remains constant, the entropy is removed from the spin system and goes into the lattice, which lowers the magnetic entropy and produces a net heat. To this sample La-deficiency in oxygen nonstoichiometry without the divalent alkali ions injection of this phase, the amount of lattice is lack of La vacancies samples, so the total value of the magnetic entropy change corresponding to a magnetic field variation of 1 T for the $\text{La}_{0.7}\text{MnO}_{3-\delta}$ is still about -1.32 J/kg K and the refrigerant capacity is approximately close to 37 J/kg at 1 T magnetic field, though it is less than that of other series of T_C around room temperature of perovskites manganites material [28].

La-deficient bulk perovskite manganite $\text{La}_{0.7}\text{MnO}_{3-\delta}$ has the advantages of easy fabrication and higher chemical stability,

etc., and its large magnetic entropy changes are closer to room temperature. The above-mentioned merits make it a likely suitable candidate as a working substance in magnetic refrigeration technology.

The work was supported by the National Laboratory of Solid State Microstructure of Nanjing University (LSSMS) under Grant No. M23005, and Department of personnel Jiangsu Six Talent Fund under Grant No. AD41118.

References

- [1] J.E. Gordon, S.D. Bader, J.F. Mitchell, R. Osborn, S. Rosenkranz, Phys. Rev. B 60 (1999) 6258.
- [2] Z.B. Guo, J.R. Zhang, H. Huang, W.P. Ding, Y.W. Du, Appl. Phys. Lett. 70 (1997) 904.
- [3] Z.B. Guo, Y.W. Du, J.S. Zhu, H. Huang, W.P. Ding, D. Feng, Phys. Rev. Lett. 78 (1997) 1142.
- [4] K. Ghosh, R.L. Greene, S.E. Lofland, S.M. Bhagat, S.G. Karabashev, D.A. Shulyatev, A.A. Arsenov, Y. Mukovskii, Phys. Rev. B 58 (1998) 8206.
- [5] Tie-Jun Zhou, Z. Yu, W. Zhong, X.N. Xu, H.H. Zhang, Y.W. Du, J. Appl. Phys. 85 (1999) 7975.
- [6] Q.Y. Xu, K.M. Gu, X.L. Liang, G. Ni, Z.M. Wang, H. Sang, Y.W. Du, J. Appl. Phys. 90 (2001) 524.
- [7] Manh-Huong Phan, Seong-Cho Yu, Nam Hwi Hur, Yoon-Hee Jeong, J. Appl. Phys. 96 (2004) 1154.
- [8] A.N. Ulyanov, Y.M. Kang, S.I. Yoo, J. Appl. Phys. 103 (2008) 07B328.
- [9] D.N.H. Nam, N.V. Dai, L.V. Hong, N.X. Phuc, S.C. Yu, M. Tachibana, E. Takayama-Muromachi, J. Appl. Phys. 103 (2008) 043905.
- [10] J. Yang, Y.P. Lee, Y. Li, J. Appl. Phys. 102 (2007) 033913.
- [11] Manh-Huong Phan, Nguyen Duc Tho, Nguyen Chau, Seong-Cho Yu, M. Kurisu, J. Appl. Phys. 97 (2005) 103901.
- [12] A.M. Gomes, F. Garcia, A.P. Guimarães, M.S. Reis, V.S. Amaral, Appl. Phys. Lett. 85 (2004) 4974.
- [13] X. Bohigas, J. Tejada, E. Del Barco, X.X. Zhang, M. Sales, Appl. Phys. Lett. 73 (1998) 390.
- [14] D.T. Morelli, A.M. Mance, J.V. Mantese, A.L. Micheli, J. Appl. Phys. 79 (1996) 373.
- [15] Y. Sun, X.J. Xu, Y.H. Zhang, J. Magn. Magn. Mater. 219 (2000) 183.
- [16] Z.M. Wang, G. Ni, H. Sang, Y.W. Du, J. Magn. Magn. Mater. 234 (2001) 213.
- [17] X.X. Zhang, J. Tejada, Y. Xin, G.F. Sun, K.W. Wong, X. Bohigas, Appl. Phys. Lett. 69 (1996) 3596.
- [18] S. Pignard, H. Vincent, J.P. Senateur, K. Frohlich, J. Souc, Appl. Phys. Lett. 73 (1998) 999.
- [19] A. Gupta, T.R. Mcguire, P.R. Duncombe, M. Rupp, J.Z. Sun, W.J. Gallagher, G. Xiao, Appl. Phys. Lett. 67 (1995) 3494.
- [20] H. Vincent, S. Pignard, J.P. Senateur, J. Pierre, J. Magn. Magn. Mater. 177–181 (1998) 1227.
- [21] S.S. Manoharan, D. Kumar, M. Hegde, J. Solid State Chem. 117 (1995) 420.
- [22] S. Pignard, H. Vincent, J.P. Senateur, J. Pierre, A. Abrutis, J. Appl. Phys. 82 (1997) 4445.
- [23] B.C. Hauback, H. Fjellvag, N. Sakai, J. Solid State Chem. 124 (1996) 43.
- [24] P.A. Joy, C. Raj Sankar, S.K. Date, J. Phys: Condens. Matter 14 (2002) L663.
- [25] J. Topfer, J.B. Goodenough, Chem. Mater. 9 (1997) 1467.
- [26] V.K. Pecharsky, K.A. Gschneidner, A.O. Tsokol, Rep. Prog. Phys. 68 (2005) 1479.
- [27] V.K. Pecharsky, K.A. Gschneidner, Annu. Rev. Mater. Sci. 30 (2000) 387.
- [28] M.H. Phan, S.C. Yu, J. Magn. Magn. Mater. 308 (2007) 325.
- [29] N.S. Bingham, M.H. Phan, H. Srikanth, M.A. Torjica, C. Leighton, J. Appl. Phys. 106 (2009) 023909.
- [30] B.K. Banerjee, Phys. Lett. 12 (1964) 16.
- [31] J. Mira, J. Rivas, F. Rivadulla, C. Vazquez-Vazquez, M.A. Lopez-Quintela, Phys. Rev. B 60 (1999) 2998.
- [32] E. Dagotto, T. Hotta, A. Moreo, Phys. Rep. 344 (2001) 1.

- [33] A. Arulraj, R. Mahesh, G.N. Subbanna, R. Mahendiran, A.K. Raychauri, C.N.R. Rao, *J. Solid State Chem.* 127 (1996) 87.
- [34] G.J. Chen, Y.H. Chang, H.W. Hsu, *J. Magn. Magn. Mater.* 219 (2000) 317.
- [35] S. Pignarda, K. Yu-Zhangb, Y. Leprince-Wangb, K. Hanc, H. Vincenta, J.P. Senateur, *Thin Solid Films* 391 (2001) 21.
- [36] M. Patra, K. De, S. Majumdar, S. Giri, *Appl. Phys. Lett.* 94 (2009) 092506.
- [37] F.J. Palomares, F. Pigazo, J.J. Romero, R. Cuadrado, A. Arroyo, M.A. García, A. Hernando, R. Cortés-Gil, J.M. González-Calbet, M. Vallet-Regí, J.M. González, J.M. Alonso, *J. Appl. Phys.* 99 (2006) 08A702.
- [38] P.A. Joy, C. Raj Sankar, S.K. Date, *J. Phys: Condens. Matter* 14 (2002) 4985.
- [39] C. Ritter, M.R. Ibarra, J.M. De Teresa, P.A. Algarabel, C. Marquina, J. Blasco, J. Garcia, S. Oseroff, S.W. Cheong, *Phys. Rev. B* 56 (1997) 8902.
- [40] A.J. Millis, R. Mueller, B.I. Shraiman, *Phys. Rev. B* 54 (1996) 5405.